Relations of Counterface Hardness with Wear Behavior and Tribo-Oxide Layer of AISI H13 Steel

Q.Y. ZHANG, S.Q. WANG, X.X. LI, Y. ZHOU, K.M. CHEN, and X.H. CUI

Dry sliding wear tests of AISI H13 steel (50 HRC) against AISI D2 steel counterface with three hardness levels (55, 50, and 42 HRC) were performed at 298 K to 873 K (25 °C to 600 °C). The relations of counterface hardness with the wear behavior and tribo-oxide layer of AISI H13 steel were explored. When sliding against the different-hardness counterface, H13 steel presents appreciably changed wear behavior as a function of temperature. For H_d/H_p (the hardness ratio of disk to pin) > 1, the wear rate increases with the increase of temperature, but the wear rate variation is roughly inversed for $H_d/H_p < 1$. For $H_d/H_p = 1$, the wear rate first decreases to reach the lowest value at 473 K (200 °C) and then rapidly increases with the increase of temperature. The lowest wear rate appears at 298 K (25 °C) for $H_d/H_p > 1$, at 474 K (200 °C) for $H_d/H_p = 1$, and at 673 K (400 °C) for $H_d/H_p < 1$. As no-oxide tribolayer exists below 473 K (200 °C), the wear behavior roughly complies with Archard's equation; adhesive and abrasive wear prevail, regardless of H_d/H_p. As tribo-oxide layer exists at 473 K (200 °C) or above, the wear behavior depends on the tribo-oxide layer and thermal strength of the substrate, *i.e.*, the stability of the tribo-oxide layer. Oxidative mild wear prevails at 473 K to 873 K (200 °C to 600 °C) for $H_d/H_p < 1$ and merely at 473 K (200 °C) for $H_d/H_p = 1$. However, a mild-to-severe transition of oxidative wear occurs at 473 K to 873 K (200 °C to 600 °C) for $H_d/H_p > 1$ and at 673 K to 873 K (400 °C to 600 °C) for $H_d/H_p = 1$. These findings suggest that the tribo-oxide layers are liable to exist stably for $H_d/H_p \leq 1$ but to readily delaminate for $H_d/H_p > 1$.

DOI: 10.1007/s11661-016-3689-y

I. INTRODUCTION

FOR a given sliding system, the wear loss of sliding materials is a function of the normal force, their relative velocity, their initial temperature, and the thermal, mechanical, and chemical properties of the sliding materials.[1] This means that the wear behavior depends on various sliding conditions as well as the properties of sliding and counterface materials. The effects of sliding conditions and properties or microstructures of sliding material on the wear behavior and mechanism have been well documented.[2–12] However, the research on the effect of counterface material properties is relatively less.[13–17]

Early in 1956, Archard and Hirst proposed an empirical formula, $V = kLS/H$, where V is the wear volume, k is the wear coefficient (constant), L is the sliding distance, S is the load, and H is the hardness of softer material for a sliding pair.[2] When other parameters are definite, the wear is inversely proportional to the hardness of softer material. Clearly, it was assumed that only the material properties of the softer body influence the wear behavior of contacting surfaces. In other words, Archard's equation involves only the hardness of the softer body, without considering that of the harder one. The softer body has been taken as the only property of sliding bodies to predict the wear behavior of the tribological system for a long time.[16]

However, different views were put forward afterward. Bian *et al.* studied the unlubricated sliding wear of steels and explored the role of the hardness of the friction pair.[13] They considered that the wear rate of a pin depended mainly on the hardness of the counterface and showed very little if any dependence on its own hardness. They supposed that the wear rate of a pin was determined by the properties of tribolayer—a hot, heavily deformed mixture that bears little relationship to the original quenched-and-tempered structure, but on the hardness of the counter surface. However, Akagaki and Rigney considered that the properties of both sliding and counterface materials would affect the wear behavior.[14] They established an H_d/H_p value (a hardness ratio of counterface disk to sliding pin) as a critical factor to determine the mild-severe wear transition. When the range of hardness ratio H_d/H_p after the test included values below about 1.0, severe wear occurred. When it included only values above about 1.0, mild wear occurred. For the initial hardness ratio $H_d/H_p > 1$, the critical distance was longer for a larger initial hardness ratio.

Viáfara and Sinatora studied the influence of hardness of the harder body on the wear regime transition in a sliding pair of steels.[15] Their results confirmed the occurrence of a mild-severe wear transition when the disk hardness was decreased. They considered that a

Q.Y. ZHANG, Y. ZHOU, and X.X. LI, Ph.D. Students, K.M. CHEN and X.H. CUI, Associate Professors, and S.Q. WANG, Professor, are with the School of Materials Science and Engineering, Jiangsu University, Zhenjiang 212013, China. Contact e-mail: shuqi_wang@ujs.edu.cn, shuqi_wang@ujs.edu.cn
Manuscript submitted August 28, 2015.
Article published online September 8, 2016

predominantly elastic or plastic contact, characterized by H_d/H_p values higher or lower than 1, resulted in a mild or severe wear regime operation, respectively. Hence, H_d/H_p was used as a criterion to establish the nature of surface contact deformation and to determine the wear regime transition. It is clear that their view is in agreement with the criterion proposed by Akagaki and Rigney.[14] Recently, Viáfara and Sinatora further confirmed that the wear regime transitions were promoted by the variation in disc hardness (the harder sliding body).[16] In the high pin hardness conditions, a decrease in the disc hardness promoted the severe wear regime operation prior to the action of a mild wear regime. In the low pin hardness conditions, a severe wear regime was established. When the harder disc was tested, a mild wear regime was observed.

However, the aforementioned studies were performed at room temperature. Roy *et al.* studied the effect of mating surface on the high-temperature wear of 253 MA alloys.[17] They pointed out that the wear behavior of metallic material was governed by the hardness and oxidation kinetics of the mating surface. In air, the presence of a transfer layer, mechanically mixed layer, and composite layer was considered to govern the wear behavior, particularly at elevated temperature. The chemical characteristics of these layers were dependent on the test temperature and the counterface material. Roy *et al.*'s viewpoint seemed to comply with Bian *et al.*'s[13] hypothesis.

From all the former research on the effect of counterface hardness on wear, three main results can be summarized: (1) counterface hardness presented more obvious influences on the wear behavior of pin even than hardness itself; (2) H_d/H_p or the relative hardness of sliding and counterface materials indeed presented some relations with wear regimes, but these results were not total conformity; and (3) the effect of counterface hardness on wear seemed to be closely related with tribolayers. However, the relations of counterface hardness with dry sliding wear behavior and tribo-oxide layers are still unclear.

In the present study, the effect of the counterface hardness on the wear behavior of H13 steel was thoroughly investigated from 298 K to 873 K (25 °C to 600 °C) using a pin-on-disc wear tester. AISI D2 steel as the counterface was heat treated to reach three hardness levels of 55, 50, and 42 HRC, which were harder, comparable, and softer compared to H13 steel (50 HRC), respectively. The phase, morphology, composition, and microhardness of the worn surface and subsurface of H13 steel were wholly examined. The relations of counterface hardness with wear behavior and tribo-oxide layers were clarified; the wear mechanism was explored as well.

II. EXPERIMENTAL DETAILS

Commercial AISI H13 steel (Fe-0.41 pct C-5.23 pct Cr-1.15 pct Mo-0.92 pct V-1.04 pct Si-0.43 pct Mn) and AISI D2 steel (Fe-1.2 pct C-11.85 pct Cr-0.46 pct Mo-0.25 pct V-0.34 Si-0.37 pct Mn) were selected for pin and disk specimens, respectively. The flat-end pins were of 6-mm diameter and 12-mm height; the disks were of 70-mm diameter and 10-mm thickness. The H13 and D2 steel were austenitized at 1313 K (1040 °C) and 1423 K (1150 °C) for 20 minutes, respectively, and then quenched in oil. The austenitized H13 steel was tempered at 473 K (200 °C) for 2 hours and cooled in air to achieve mainly tempered martensite and a hardness of 50 HRC. The austenitized D2 steel was tempered twice at 823 K, 853 K, and 903 K (550 °C, 580 °C, and 630 °C) for 2 hours to achieve mainly tempered troostite (55 HRC), tempered troostite plus sorbite (50 HRC), and tempered sorbite (42 HRC), respectively. In these cases, the hardness ratios of disk to pin (H_d/H_p) were equal to 1.1 (>1), 1 (=1), and 0.84 (<1), respectively.

Dry sliding wear tests were performed in air on an MG-2000 type pin-on-disk high-temperature wear tester according to the standard of ASTM G 99-05. The counterface disk was fixed on a rotating lower shaft; the pin specimen was installed with a holder attached on a static upper spindle by a screw and then pressed against the disk under a vertical load by a dead weight. This wear-test apparatus is equipped with a 2-KW resistance heater to obtain an ambient temperature up to 873 K (600 °C). The sliding parameters were determined as follows: 298 K, 473 K, 673 K, and 873 K (25 °C, 200 °C, 400 °C, and 600 °C) for the ambient temperatures (testing temperatures), 50 to 300 N with an interval of 50 N for the normal load, 1 m/s for the sliding velocity, and 1200 m for the sliding distance. Prior to each test, both of the pins and disks were ground with 600# silicon carbide paper to achieve a R_a of 0.38 mm and then ultrasonically cleaned in acetone and dried. The wear loss of pin was determined by mass measurement before and after a test by an electric balance with an accuracy of 0.01 mg. The wear rate was calculated by the following formula: $W = \Delta M/\rho L$, where ΔM is the wear loss of the pin, ρ is the density of H13 steel, and L is the sliding distance. The mean value and error bar of three repeated tests were provided. A growth rate (K) of wear rate from 250 to 300 N was defined as the difference of wear rate under the unit load, $K = (W_{300} - W_{250})/50$, where W_{250} and W_{300} are the values of wear rate under 250 and 300 N, respectively.

The phases on the worn surfaces were identified by a D/Max-2500/pc type X-ray diffractometer with Cu K_α radiation. The morphology and composition of worn surfaces and subsurfaces were examined by a JSM-7001F type scanning electron microscope and an Inca Energy 350 type energy dispersion spectrometer, respectively. The microhardness distribution in the cross section of worn surfaces was measured by an HVS-1000 type digital microhardness tester. The hardness of as-treated steels was measured by an HR-150A type Rockwell apparatus.

III. RESULTS AND DISCUSSION

A. *Wear Behavior*

The wear rate curves of H13 steel sliding against the different-hardness counterface are presented in Figure 1.

The growth rate of wear rate from 250 to 300 N is summarized in Table I. H13 steel presents appreciably changed wear behavior as a function of temperatures during sliding against the different-hardness counterface. For H_d/H_p = 1.1 (Figure 1(a)), the wear rate of H13 steel increases with an increase of load and temperature. At 298 K to 673 K (25 °C to 400 °C), the wear rate marginally increases under 50 to 250 N but rapidly increases under 250 to 300 N. At 873 K (600 °C), however, the wear rate always increases rapidly. The growth rate of wear rate represents an increasing tendency of wear rate under high load from 250 to 300 N. As shown in Table I, the wear rate at $H_d/H_p > 1$ presents a low growth rate at room temperature but a high one at elevated temperatures. On the contrary, $H_d/H_p < 1$ results in a high growth rate at room temperature but a low, even minus, one at elevated temperatures.

For H_d/H_p = 1 (Figure 1(b)), the wear rate first decreases to reach the lowest value at 473 K (200 °C) and then rapidly increases with an increase of temperature. Compared with the former, the growth rate of wear rate seems to decrease dramatically and reach the lowest value (0.004) at 473 K (200 °C) (Table I). For

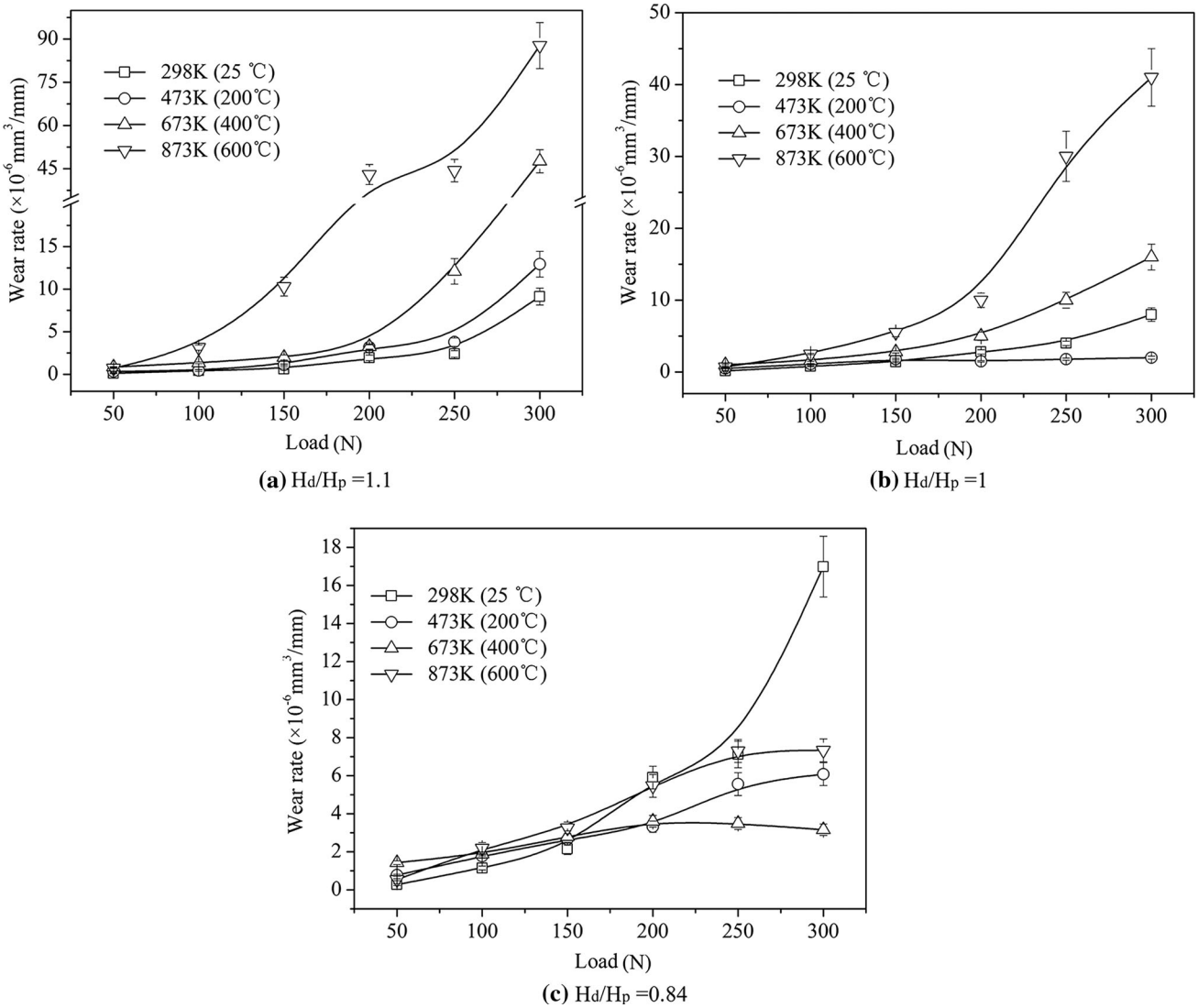

Fig. 1—Wear rate curve of H13 steel for different H_d/H_p: (*a*) H_d/H_p = 1.1, (*b*) H_d/H_p = 1, and (*c*) H_d/H_p = 0.84.

Table I. Growth Rate ($mm^3\ mm^{-1}\ N^{-1}$) of Wear Rate from 250 to 300 N under Various Temperatures

Hardness Ratio (H_d/H_p)	298 K (25 °C)	473 K (200 °C)	673 K (400 °C)	873 K (600 °C)
1.1	0.135	0.183	0.710	0.869
1	0.081	0.004	0.120	0.220
0.84	0.197	0.010	−0.007	0.001

H_d/H_p = 0.84 (Figure 1(c)), the wear rate roughly decreases with an increase of temperature. The wear rate first decreases with a temperature from 298 K to 673 K (25 °C to 400 °C), then slightly increases from 673 K to 873 K (400 °C to 600 °C), and reaches its lowest value at 673 K (400 °C). The curve at 298 K (25 °C) presents a higher growth rate of wear rate than those at elevated temperatures, especially at 673 K (400 °C). It must be noted that the growth rate at 673 K (400 °C) is −0.007, a negative growth of wear rate, as shown in Table I.

As mentioned previously, the counterface hardness totally changes the wear behavior of H13 steel as a function of temperature. To reveal the relations among the wear rate, temperature, and H_d/H_p, the wear rate of H13 steel sliding against three-hardness counterfaces is plotted at various temperatures in Figure 2. At 298 K (25 °C), the wear rate roughly decreases with the increase of H_d/H_p and vice versa at 673 K to 873 K (400 °C to 600 °C). Below 200 N at 473 K (200 °C), the same variation law with H_d/H_p appears as at 298 K (25 °C). However, under above 200 N, the wear rate first decreases to reach the lowest value for H_d/H_p = 1 and then markedly increases with the increase of H_d/H_p.

As H_d/H_p is more than 1, H13 steel possesses a better room-temperature wear resistance but a terrible high-temperature wear resistance, especially at 673 and 873 K (400 and 600 °C). However, as H_d/H_p decreases, the room-temperature wear resistance worsens. Instead the high-temperature wear resistance is markedly improved, as shown in Figures 2(a), (c), and (d). Clearly, a wear transition as a function of H_d/H_p seems to occur at a critical temperature of 473 K (200 °C) (Figure 2(b)). The lowest wear rate and the best wear resistance appear at 298 K (25 °C) for $H_d/H_p > 1$, at 473 K (200 °C) for H_d/H_p = 1, and at 673 K to 873 K (400 °C to 600 °C) for $H_d/H_p < 1$. To explore the reason for wear transition and expound the wear mechanism, the wear characteristics of H13 steel in the extreme conditions, H_d/H_p = 1.1 and H_d/H_p = 0.84, were focused on in the investigation, in terms of the phase, morphology, composition, and microhardness of worn surfaces and subsurfaces.

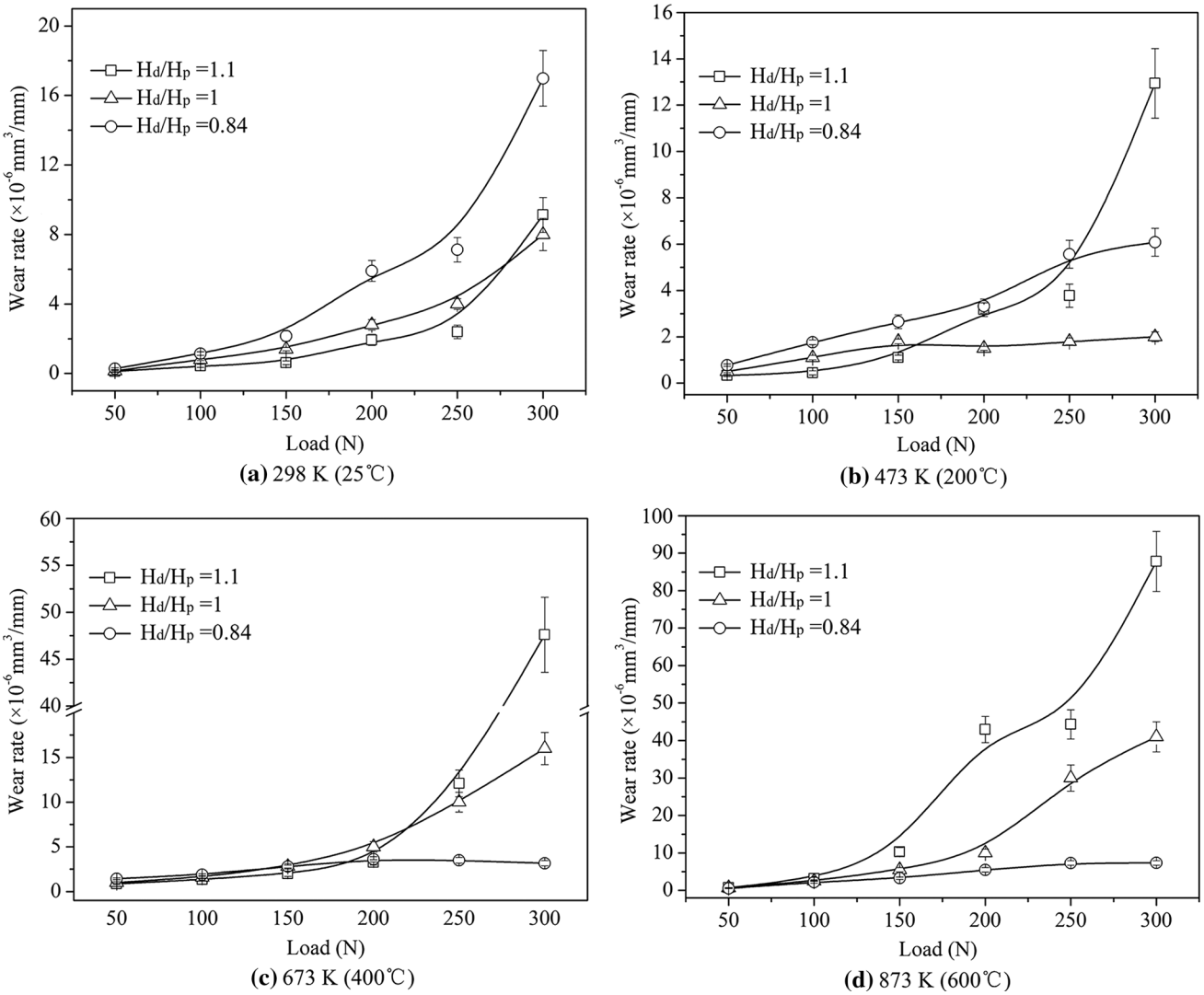

Fig. 2—Wear rate of H13 steel for three hardness ratios at various temperatures: (*a*) 298 K (25 °C), (*b*) 473 K (200 °C), (*c*) 673 K (400 °C), and (*d*) 873 K (600 °C).

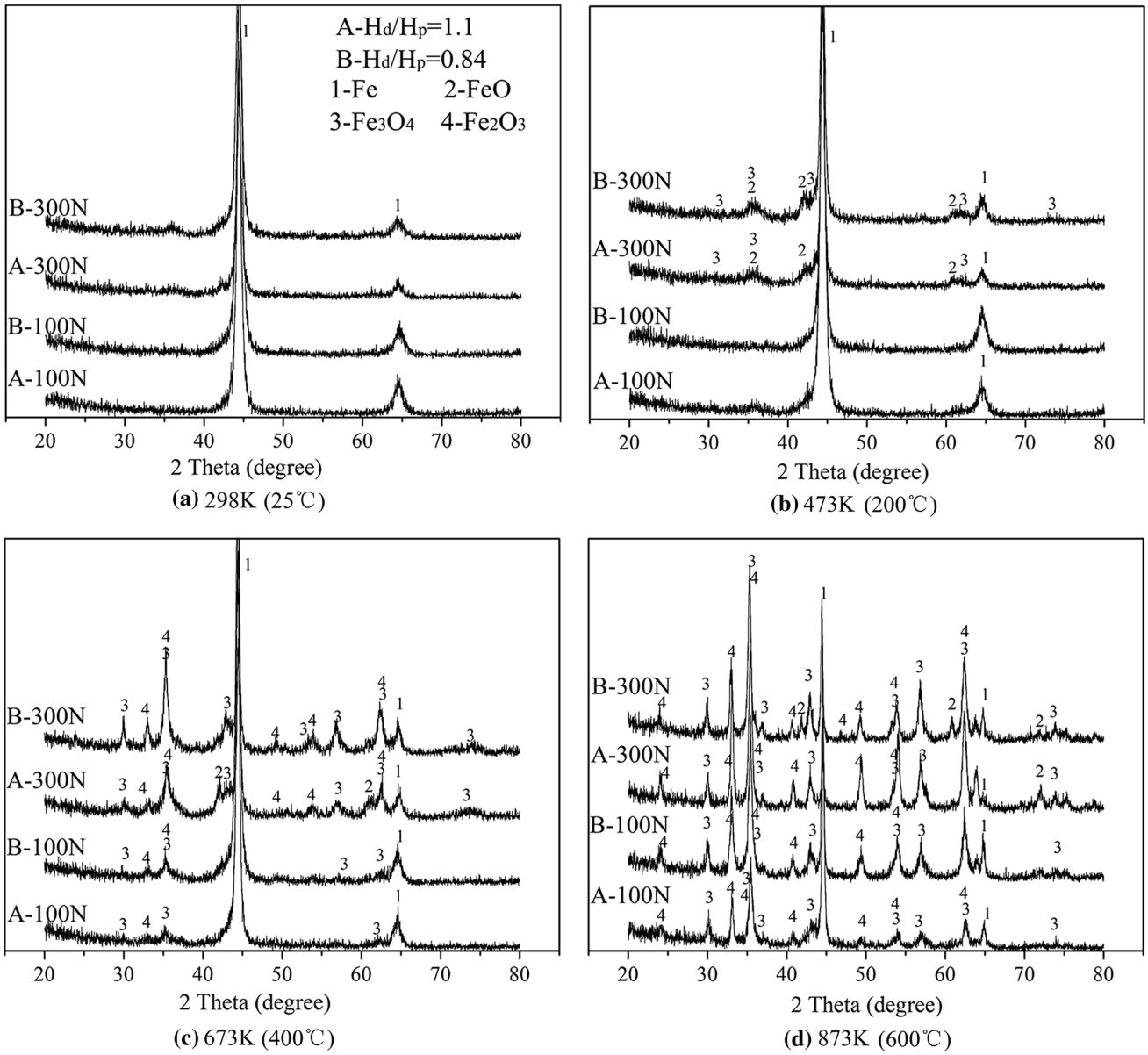

Fig. 3—XRD patterns for worn surfaces of H13 steel at various temperatures: (*a*) 298 K (25 °C), (*b*) 473 K (200 °C), (*c*) 673 K (400 °C), and (*d*) 873 K (600 °C).

B. *Analysis of Worn Surfaces and Subsurfaces*

1. *X-ray diffraction patterns of worn surfaces*

Figure 3 illustrates X-ray diffraction (XRD) patterns for worn surfaces of H13 steel at various temperatures. At 298 K (25 °C), whether the counterface is hard or soft, the patterns are similar, as shown in Figure 3(a). There exists only Fe and almost no oxide for H_p/H_d of 1.1 and 0.84. At 473 K (200 °C), the oxide peaks start to be visible under 300 N (Figure 3(b)). As the temperature is further elevated, the amount of oxide rapidly increases (Figures 3(c) and (d)). These peaks even surpass those of Fe at 873 K (600 °C) (Figure 3(d)). This means that a great amount of tribo-oxides form and remain on worn surfaces. The higher the temperature is, the greater the tribo-oxides are. It must be noted that the oxide peak seems to be more intense for $H_d/H_p = 0.84$ than for $H_d/H_p = 1.1$ at elevated temperatures, especially under 300 N at 673 K (400 °C). This indicates that tribo-oxides readily remain on worn surfaces of H13 steel sliding against a softer counterface.

2. *Morphology of worn surface*

The worn-surface morphologies of H13 steel for H_p/H_d of 1.1 and 0.84 are illustrated in Figures 4 and 5, respectively. Under 100 N at 298 K and 473 K (25 °C and 200 °C), there is almost no difference on the worn surfaces of H13 steel, regardless of the counterface hardness. A large number of grooves, fish scale, and tearing traces along the sliding track are distinctly identified (Figures 4 and 5(a) through (c)). These are the typical characteristics of abrasive and adhesive wear. Additionally, scattered particles on worn surfaces seem

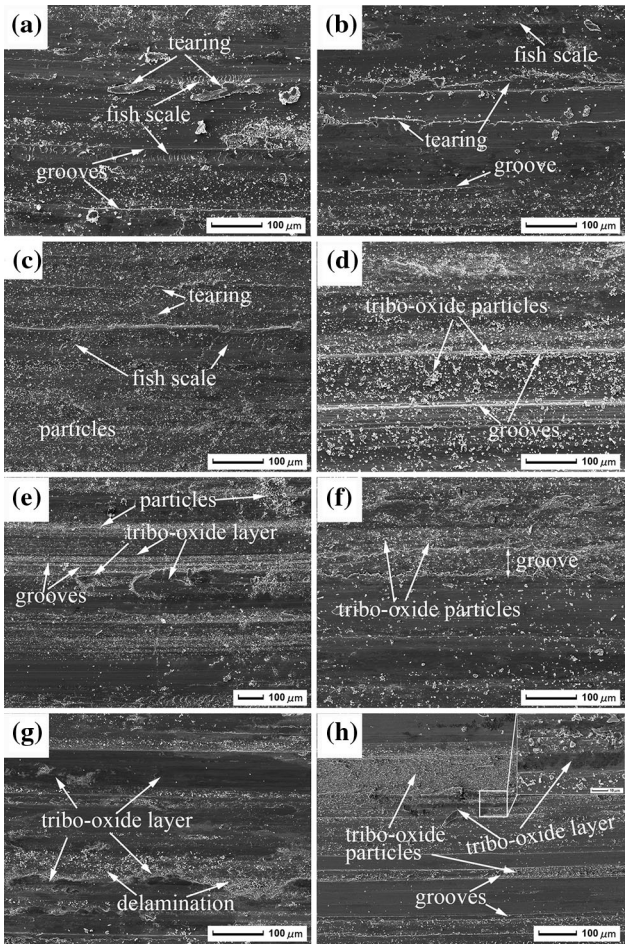

Fig. 4—Worn-surface morphology of H13 steel for $H_d/H_p = 1.1$: (*a*) 100 N, 298 K (25 °C); (*b*) 300 N, 298 K (25 °C); (*c*) 100 N, 473 K (200 °C); (*d*) 300 N, 473 K (200 °C); (*e*) 100 N, 673 K (400 °C); (*f*) 300 N, 673 K (400 °C); (*g*) 100 N, 873 K (600 °C); and (*h*) 300 N, 873 K (600 °C).

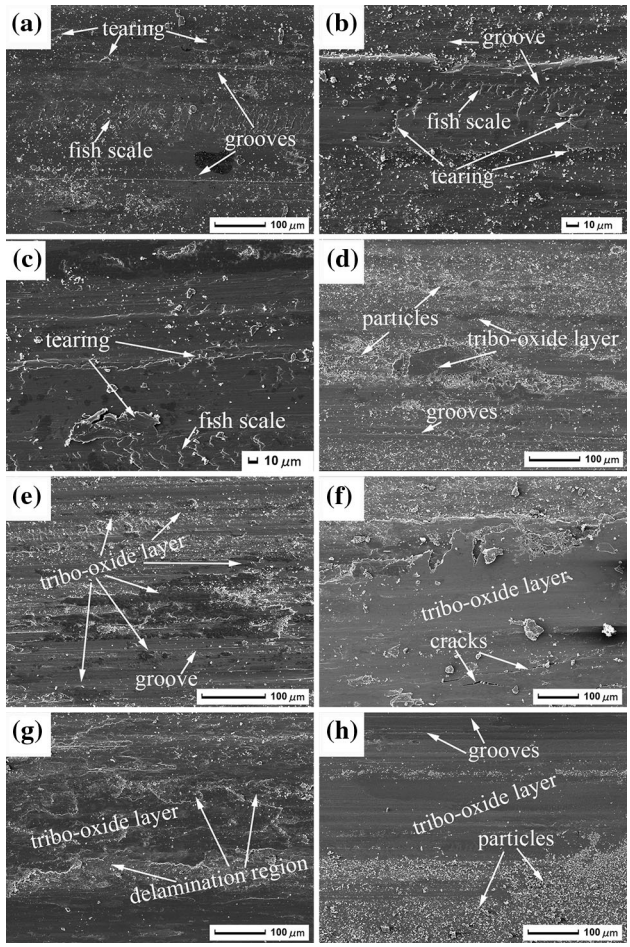

Fig. 5—Worn-surface morphology of H13 steel for $H_d/H_p = 0.84$: (*a*) 100 N, 298 K (25 °C); (*b*) 300 N, 298 K (25 °C); (*c*) 100 N, 473 K (200 °C); (*d*) 300 N, 473 K (200 °C); (*e*) 100 N, 673 K (400 °C); (*f*) 300 N, 673 K (400 °C); (*g*) 100 N, 873 K (600 °C); and (*h*) 300 N, 873 K (600 °C).

to be some oxides. However, in this case, the amount of oxides is too small to be identified by XRD.

When the temperature is elevated, significantly different worn-surface morphologies are noticed, as shown in Figures 4 and 5. The adhesive characteristics seem to wholly disappear on worn surfaces; instead, a black and smooth worn surface appears accompanied with some delaminated regions. In these cases, XRD can identify oxides. Hence, tribo-oxides can be confirmed to exist. For $H_d/H_p = 1.1$, at 473 K (200 °C), tribo-oxide layers seem not to form but a small amount of oxides exist as scattering particles. As the temperature reaches 673 K (400 °C), the tribo-oxide layers start to appear in the form of black and smooth patches and then expand somewhat under 100 N from 673 K to 873 K (400 °C to 600 °C) (Figures 4(e) and (g)). However, under a heavy load (300 N), tribo-oxide layers abruptly disappear. In this case, oxide particles and deep grooves emerge on worn surfaces (Figures 4(f) and (h)). Some oxide particles are observed to congregate in grooves, as shown in Figure 4(h). The same case is noticed to appear under 300 N at 473 K (200 °C) (Figure 4(d)).

From the XRD results, more oxides exist on worn surfaces for $H_d/H_p = 0.84$, compared with those in the same cases for $H_d/H_p = 1.1$. For $H_d/H_p = 0.84$, tribo-oxide layers start to appear under 300 N at 473 K (200 °C). As the temperature increases, the layers seem to become more continuous and compact, as shown in Figures 5(e) and (g). Particularly, the area of the black, smooth tribo-oxide layers markedly enlarges. As the load reaches 300 N, the area of the tribo-oxide layer further extends at 473 K, 673 K, and 873 K (200 °C, 400 °C, and 600 °C) (Figures 5(d), (f), and (h)), accompanied with a small number of cracks and narrower grooves. The tribo-oxide layers almost cover the entire worn surface at 673 K and 873 K (400 °C and 600 °C). Interestingly, these phenomena never happen for $H_d/H_p = 1.1$. In addition, some oxide particles appear, but merely scatter on the worn surface rather than mainly congregate in the grooves. The latter case occurs for $H_d/H_p = 0.84$, as shown in Figure 5(h).

3. *Cross-section morphology of worn surfaces and subsurfaces*

From the cross-section morphology of worn surfaces and subsurfaces, the tribolayers can be identified. Figures 6 and 7 illustrate the cross-section morphology

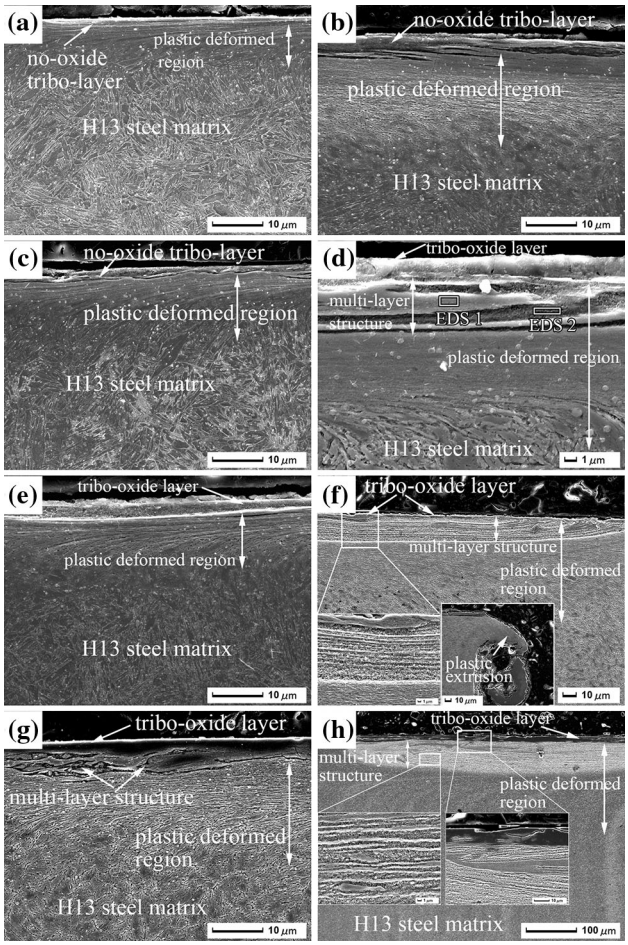

Fig. 6—Cross-section morphology of worn surfaces of H13 steel for H_d/H_p = 1.1: (*a*) 100 N, 298 K (25 °C); (*b*) 300 N, 298 K (25 °C); (*c*) 100 N, 473 K (200 °C); (*d*) 300 N, 473 K (200 °C); (*e*) 100 N, 673 K (400 °C); (*f*) 300 N, 673 K (400 °C); (*g*) 100 N, 873 K (600 °C); and (*h*) 300 N, 873 K (600 °C).

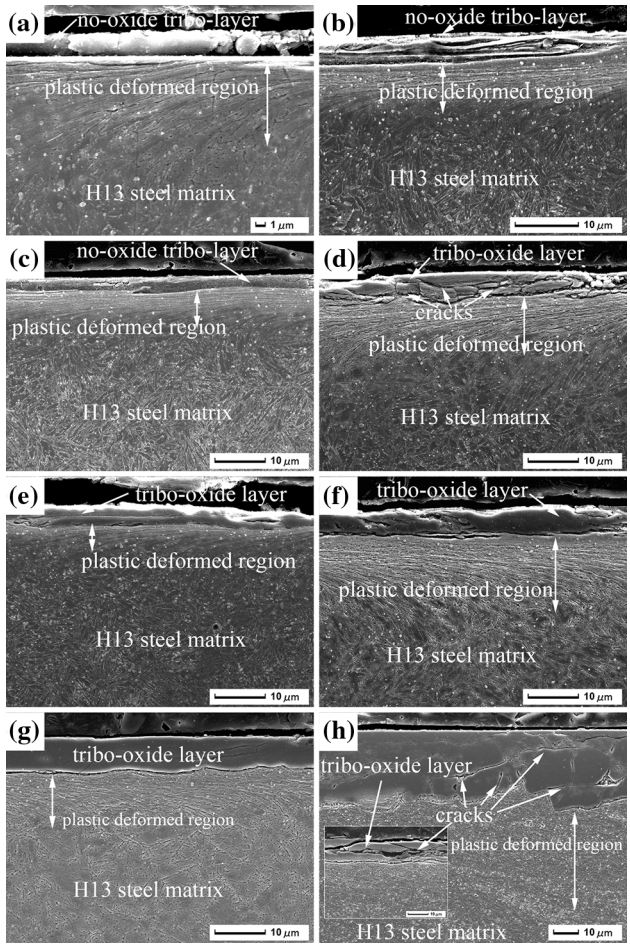

Fig. 7—Cross-section morphology of worn surfaces of H13 steel for H_d/H_p = 0.84: (*a*) 100 N, 298 K (25 °C); (*b*) 300 N, 298 K (25 °C); (*c*) 100 N, 473 K (200 °C); (*d*) 300 N, 473 K (200 °C); (*e*) 100 N, 673 K (400 °C); (*f*) 300 N, 673 K (400 °C); (*g*) 100 N, 873 K (600 °C); and (*h*) 300 N, 873 K (600 °C).

of worn surfaces and subsurfaces of H13 steel for H_p/H_d of 1.1 and 0.84, respectively. Clearly, from the worn surface to subsurface, there exist three regions successively: the tribolayer, the plastic-deformed region, and the undeformed matrix. As shown in Figures 6 and 7, tribolayers are confirmed to invariably exist in various conditions. However, tribolayers present different characteristics because of their formation conditions, *i.e.*, different temperatures and loads.

For H_d/H_p = 1.1, different morphologies are revealed under low and high load, respectively. Under 100 N, the tribolayer and plastic-deformed region are observed to always exist. At 298 K and 473 K (25 °C and 200 °C), tribolayers are thin and discontinuous, as shown in Figures 6(a) and (c), in which there are almost no oxides from XRD results. Thus, the tribolayer is essentially metallic and termed as no-oxide tribolayer. As the temperature is elevated, the tribolayer becomes thick and relatively continuous and contains many oxides. In this case, tribolayer is accounted as tribo-oxide layer (Figures 6(e) and (g)). With the load increasing to 300 N, tribo-oxide layers do not thicken, but the plastic deformation intensifies, even resulting in a severe plastic extrusion at elevated temperatures, as shown in the magnified image of Figure 6(f). Additionally, a multilayer structure is generated between the worn surface and plastic-deformed region, which is composed of some strip-shaped compound including metals and oxides according to energy dispersion spectroscopy (EDS) (Figure 8), as shown in Figures 6(d), (f), and (h). At 473 K (200 °C), the multilayer structure merely occurs in local regions (Figure 6(d)), but it rapidly spreads and covers the entire subsurface at 673 K and 873 K (400 °C and 600 °C) (Figures 6(f) and (h)). Even the multilayer structure is noticed to exist under 100 N at 873 K (600 °C) (Figure 6(g)). The microstructure of H13 steel substrate is transformed from tempered martensite to tempered troostite at 673 K (400 °C), 300 N, and tempered sorbite at 873 K (600 °C), 300 N, for H_d/H_p = 1.1, but it did not change in other conditions.

For H_d/H_p = 0.84, worn surfaces present similar morphologies to the cases at H_d/H_p = 1.1 in various conditions. Under 100 N at 298 K (25 °C) and 473 K (200 °C), no-oxide tribolayer and plastic-deformed region are observed on the upper part at subsurfaces, as shown in Figures 7(a) through (c). However, from

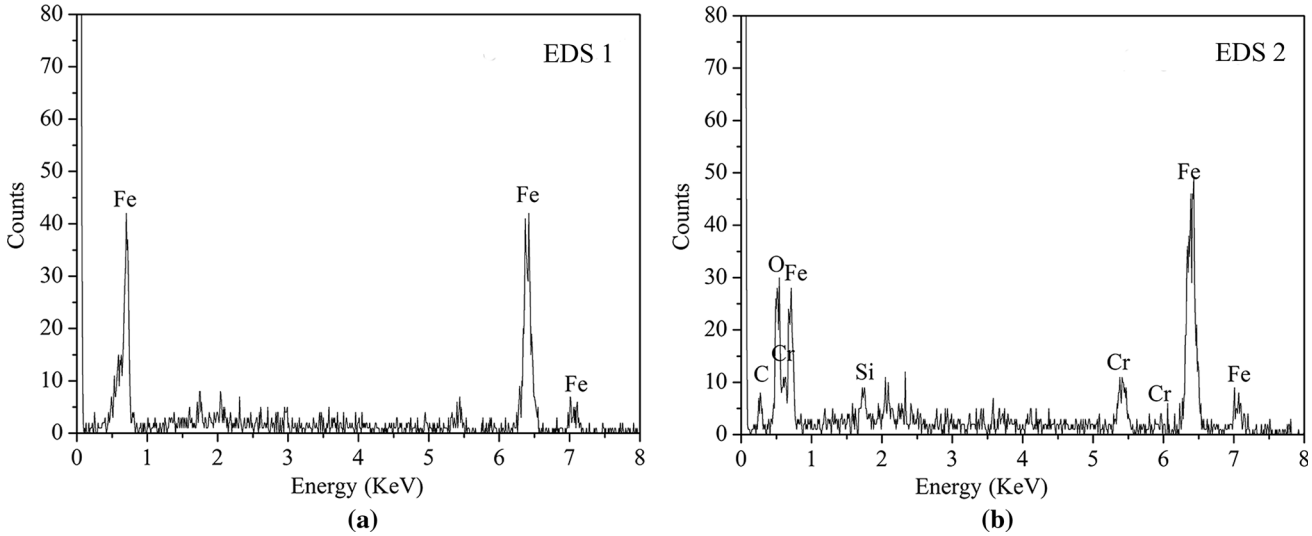

Fig. 8—EDS regional analysis in Fig. 6(d): (*a*) EDS 1 and (*b*) EDS 2.

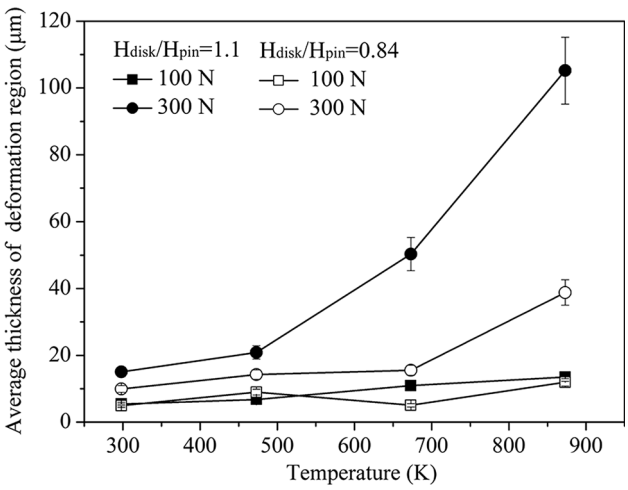

Fig. 9—Average thickness of deformation region as a function of temperature and H_d/H_p.

300 N at 473 K (200 °C), the tribolayers start to contain numerous oxides and turn into tribo-oxide layers. The tribo-oxide layers are thick, compact, and continuous as well as present almost no cracks at 673 K (400 °C) (Figures 7(e) and (f)) and 873 K (600 °C) (Figure 7(g)). However, under 300 N at 473 K and 873 K (200 °C and 600 °C), the tribo-oxide layers embrace some cracks and even peel off in certain regions (Figures 6(d) and (h)). Additionally, it must be emphasized that there is almost no multilayer structure in the cross section at subsurfaces for $H_d/H_p = 0.84$. The microstructure of H13 steel is transformed from tempered martensite to tempered sorbite, at 600 °C, 300 N, for $H_d/H_p = 0.84$.

The formation of multilayer structure is attributed to the fact that serious plastic deformation and oxides coexist on worn surfaces and at subsurfaces. Thus, during sliding, oxides are mixed with deformed matrix to form multilayer structure, *i.e.*, laminated structure alternatively containing oxides and deformed matrix. Such a tribo-oxide layer is considered to be of no load-bearing function. Thus, there occurs intensive interaction between counterface and sliding pin. The load-bearing function of tribo-oxide layers can be also guessed by the deformed region size at subsurfaces under the same load, as shown in Figure 9. Under low loads (100 N), the deformed region sizes at subsurfaces are similar to each other for different H_d/H_p. As the high load is applied, the deformed region size at subsurfaces rapidly increases. More importantly, the deformed region size at $H_d/H_p = 1.1$ is markedly higher than that at $H_d/H_p = 0.84$. A large deformed region means low load-bearing function of tribo-oxide layers. Because of the low load-bearing function of tribo-oxide layers, the friction force can be transmitted to deeper matrix and result in large plastic deformation. Compared with the low one, the high H_d/H_p presents a large plastic deformation region and even a multilayer structure appears. The main reason is that high H_d/H_p reduces the load-bearing function of the tribo-oxide layer. In other words, at high H_d/H_p, the tribo-oxide layer readily lost its soundness, thus reducing its load-bearing function. Conversely, at low H_d/H_p, the tribo-oxide layer retained its soundness, thus presenting high load-bearing function.

4. *Microhardness distribution at worn subsurface*

Figure 10 shows the microhardness distribution at worn subsurfaces of H13 steel for H_d/H_p of 1.1 and 0.84. The microhardness distribution of worn subsurfaces demonstrates the hardness of subsurface material after wear, which can be used as the evaluation for the retained strength of subsurface material. During sliding, subsurface material is plastically deformed and strengthened under the action of load, or is thermally softened by the dynamic recovery and recrystallization under action of friction heat and ambient temperature. Hence, the hardness in cross section near the worn surface presents an increase or a decrease by the synergy action of plastic deformation strengthening and thermal

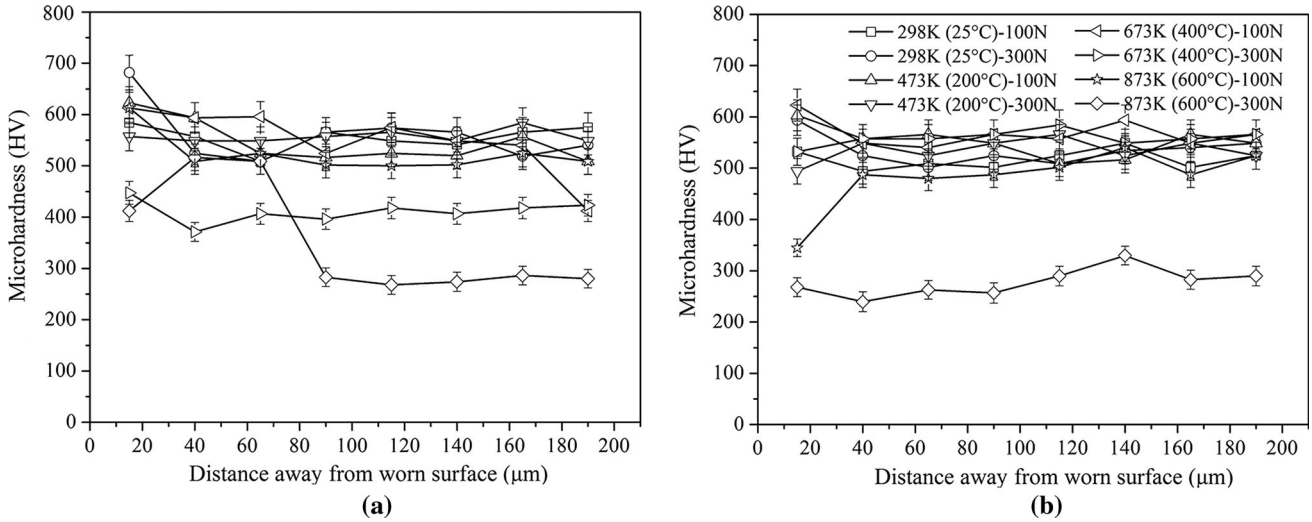

Fig. 10—Microhardness distribution of worn subsurface of H13 steel for H_d/H_p equal to (*a*) 1.1 and (*b*) 0.84.

softening during sliding. Whether the tribo-oxide layers are protective or not depends on the retained strength of subsurface material. As long as subsurface material retains enough strength, tribo-oxide layers take a protective function. Otherwise, as subsurface material does not provide a strong support for tribo-oxide layers, it readily delaminates and loses protection for the matrix underneath. In most cases, the inner hardness away from the worn surfaces tends to approach a certain value and locate in the range of 520 to 580 HV, which is the original hardness of H13 steel matrix. Even the hardness of subsurface material slightly increases at 20 μm from the worn surface. However, for $H_d/H_p = 1.1$, under 300 N, the hardness of H13 steel matrix appreciably decreased to 400 HV at 673 K (400 °C) and 260 to 300 HV at 873 K (600 °C). This means that a serious thermal softening occurs under 300 N at 673 K to 873 K (400 °C to 600 °C). In the distance of 70 μm from worn surfaces, there is an increase of hardness under 300 N at 873 K (600 °C), which may be attributed to the existence of multilayer structure.

For $H_d/H_p = 0.84$, merely under 300 N at 873 K (600 °C), a thermal softening occurs at the total subsurface, but a thermal softening only partly occurs under 100 N at 873 K (600 °C). Thus, in the distance of 40 μm from the worn surfaces, the hardness substantially decreases to 350 HV. This means that thermal softening is preferentially induced by the harder counterface in the same condition. The multilayer structure merely appears for the harder counterface at 673 K and 873 K (400 °C and 600 °C). The hardness of the multilayer structure reaches 420 to 500 HV or so, which is significantly harder than the softened matrix but slightly softer than the original H13 steel.

C. *Summary of Wear Behavior and Mechanism*

1. *Effect of H_d/H_p on wear regime*

Archard and Hirst classified wear into mild wear and severe wear for the first time.[2] However, there was no clear concept for the severe and mild wear regimes. Zhang and Alpas provided a relatively detailed value to distinguish the mild and severe wear; that is, the boundary line between mild and severe wear was 5×10^{-6} mm^3/mm for aluminum alloys.[18] However, Wang *et al.*[19] pointed out that there was no strict dividing line between mild wear and severe wear. Therefore, in the present study, (4 to 6) $\times 10^{-6}$ mm^3/mm can be roughly considered to be the boundary range between mild and severe wear. On the basis of the preceding classification of mild and severe wear regimes, the effect of H_d/H_p on wear regimes under 200 to 300 N is illustrated in Figure 11.

As shown in Figure 11(a), under 200 and 250 N at room temperature, with an increase of H_d/H_p from 0.84 to 1.1, a severe to mild wear transition occurs. That is, at $H_d/H_p \geq 1$, a mild wear prevails; at $H_d/H_p < 1$, a severe wear occurs. However, as the load reaches 300 N, a severe wear prevails regardless of H_d/H_p. Clearly, our present results roughly follow Akagaki and Rigney's criterion. However, at 673 K and 873 K (400 °C to 600 °C), an opposite law is presented against Akagaki and Rigney's criterion.[14] As H_d/H_p increases, a mild-to-severe wear occurs. That is, at $H_d/H_p \geq 1$, a severe wear prevails except for under 200 N at 673 K (400 °C). At $H_d/H_p < 1$, a mild wear appears.

2. *Relation of H_d/H_p with tribolayer*

The results and analysis in Sect. 1 indeed present obvious effects of H_d/H_p on wear behavior and wear regimes of a pin. However, how H_d/H_p affects wear behavior seems unclear. Bian *et al.* supposed that the wear rate of a pin was determined by the properties of the tribolayer.[13] Viáfara and Sinatora considered the hardness ratio as a criterion to establish the nature of surface contact deformation and to determine the wear regime transition.[15,16] All of these demonstrate that the effects of H_d/H_p on wear behavior seem to take effect by means of tribolayer. This is similar to the view of Roy *et al.*, who pointed out that the wear behavior of metallic material was governed by the types of tribolayers.[17] Clearly, the aforementioned facts concerning

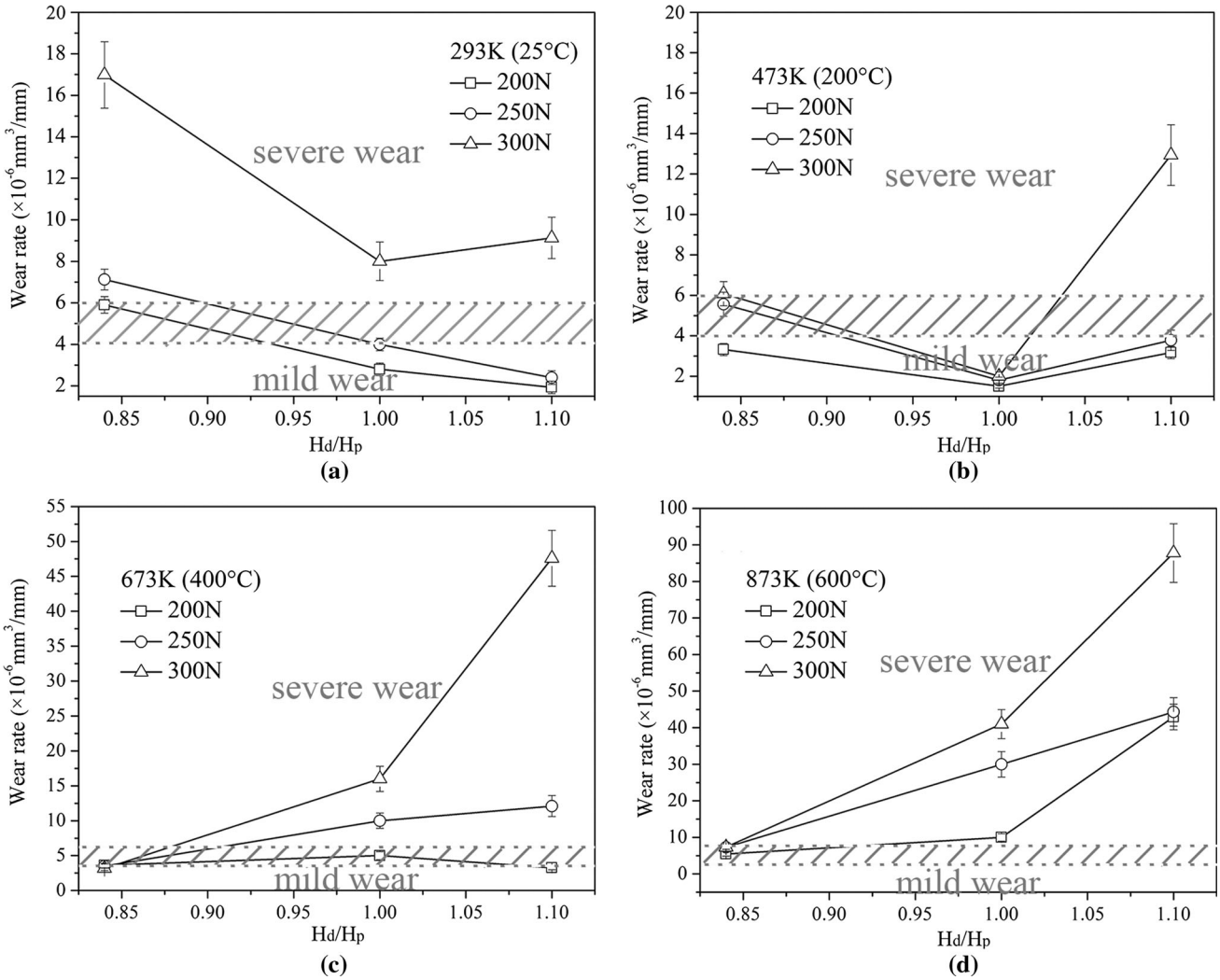

Fig. 11—Effect of H_d/H_p on wear regimes: (*a*) 298 K (25 °C), (*b*) 473 K (200 °C), (*c*) 673 K (400 °C), and (*d*) 873 K (600 °C).

Table II. Variation of Tribolayers as a Function of H_d/H_p at Various Temperatures

Temperature	$H_d/H_p > 1$	$H_d/H_p = 1$	$H_d/H_p < 1$
298 K (25 °C)	discontinuous, loose, thin; metallic; no-protective	discontinuous, loose, thin; metallic; no-protective	discontinuous, loose, thin; metallic; no-protective
473 K (200 °C)	discontinuous, loose, thin; ceramic-slightly; multi-layer; no-protective	relatively continuous, compact, thin; ceramic-slightly; mono-layer; protective	relatively continuous, compact, thin; ceramic-slightly; mono-layer; protective
673 K (400 °C)	discontinuous; ceramic; multi-layer; no-protective	discontinuous; ceramic; multi-layer; no-protective	continuous, compact, thick; ceramic; mono-layer; protective
873 K (600 °C)	discontinuous; ceramic; multi-layer; no-protective	discontinuous; ceramic; multi-layer; no-protective	continuous, compact, thick; ceramic; mono-layer; protective

Tribo-layers were characterized under 300 N at various temperatures.

the effect of H_d/H_p are pointed at tribolayers. Hence, tribolayers would be a key factor for the effect of H_d/H_p. In the present study, the variation of tribolayers as a function of H_d/H_p is summarized in Table II. The variations of tribolayers as a function of H_d/H_p can be noticed to be discontinuous, loose, thin to continuous,

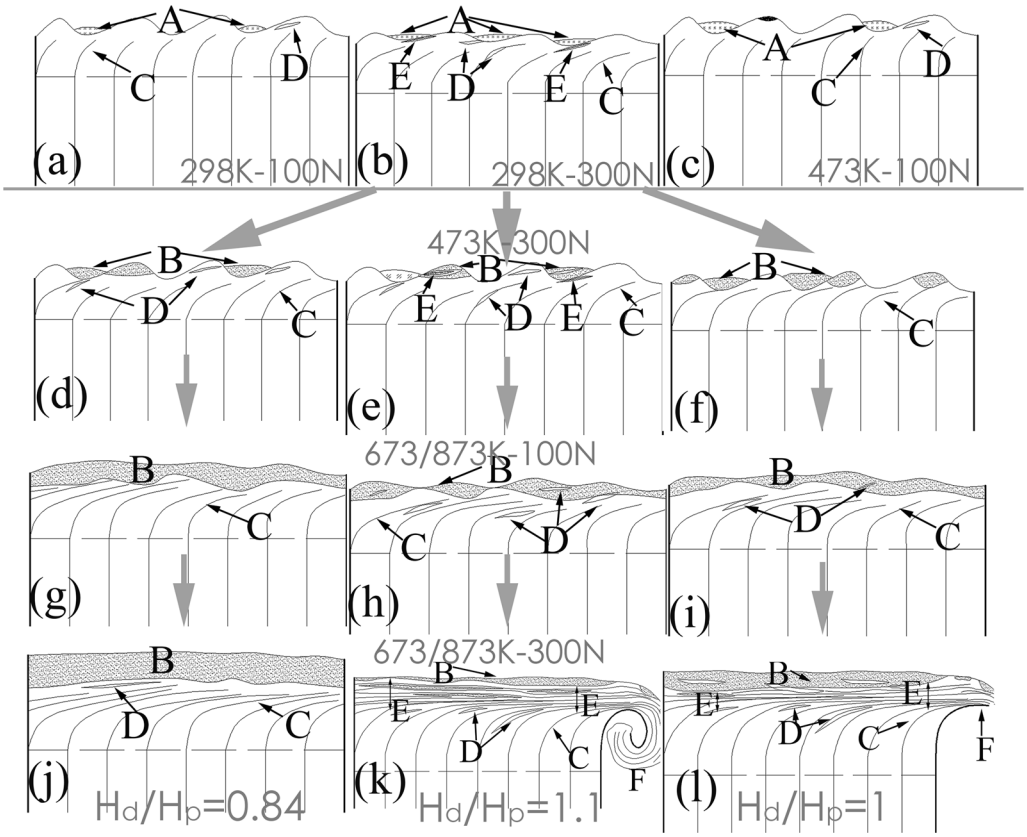

Fig. 12—Schematic model for evolution of H13 steel's tribolayer and subsurface for three hardness ratios: A—no-oxide tribolayer, B—tribo-oxide layer, C—plastic deformation, D—cracks, E—multilayer structure, and F—plastic extrusion. In the conditions of 298 K (25 °C), (*a*) 100 N and (*b*) 300 N, and (*c*) 473 K (200 °C), 100 N, there are similar wear characteristics among three ratios of H_d/H_p. In other conditions of 473 K (200 °C), 300 N, 673/873 K (400/600 °C), 100 N, and 673/873 K (400/600 °C), 300 N, the characteristics would change with variation of the hardness ratio: (*d*) 473 K (200 °C), 300 N, $H_d/H_p = 0.84$; (*e*) 473 K (200 °C), 300 N, $H_d/H_p = 1.1$; (*f*) 473 K (200 °C), 300 N, $H_d/H_p = 1$; (*g*) 673/873 K (400/600 °C), 100 N, $H_d/H_p = 0.84$; (*h*) 673/873 K (400/600 °C), 100 N, $H_d/H_p = 1.1$; (*i*) 673/873 K (400/600 °C), 100 N, $H_d/H_p = 1$; (*j*) 673/873 K (400/600 °C), 300 N, $H_d/H_p = 0.84$; (*k*) 673/873 K (400/600 °C), 300 N, $H_d/H_p = 1.1$; and (*l*) 673/873 K (400/600 °C), 300 N, $H_d/H_p = 1$. The characteristics at 673 and 873 K were similar under the same load for respective hardness ratios.

compact, thick in morphology; metallic, no-oxide to ceramic, tribo-oxide in phase; and no protection to protective in function. Because of the variations of tribolayers as a function of H_d/H_p, the changed wear behavior and mechanism are definitely expected.

According to the variation of tribolayers as a function of H_d/H_p, a schematic model of tribolayer is proposed, as shown in Figure 12. As can be seen, no-oxide tribolayer and tribo-oxide layer are formed at different conditions, respectively. The temperature of 473 K (200 °C) is a critical transition point from no-oxide tribolayer to tribo-oxide layer. As no-oxide tribolayers form on worn surfaces, the wear behaviors at different-hardness ratios are similar each other. However, as tribo-oxide layers exist, the wear behavior is markedly changed. For $H_d/H_p > 1$, the tribo-oxide layer readily delaminates and the subsurface undergoes a serious plastic deformation. On the contrary, for $H_d/H_p \le 1$, the tribo-oxide layer is liable to exist stably and the subsurface kept relatively sound, especially for $H_d/H_p = 0.84$.

At 298 K (25 °C), low ambient temperature and limited frictional heat hardly oxidize the metal surface. Under the transverse shear force, the metal-metal contact between H13 steel and the counterface results in plastic deformation, tearing of asperities junction, and generation of wear particles. Some wear particles separate from worn surfaces, and the others remain on worn surfaces.[20,21] Under normal and shear load, the retained particles are further fractured, agglomerated, and compacted at grooves. Almost no oxides can be identified by XRD. Thus, merely no-oxide tribolayer is formed on worn surfaces. In this case, no-oxide tribolayers are discontinuous, loose, only 1- to 3-μm thick, and present metallic characteristics, similar to the alloy matrix. Hence, this kind of tribolayer is considered to be no protection. Because there are more particles and grooves with the increasing load, such no-oxide tribolayers may increase somewhat in thickness and area. However, for the no protection of the no-oxide tribolayer, the increased load brings about severe plastic deformation and many cracks appear at the subsurface. This is a sign of severe wear, as previously reported.[23,24] Since there are no oxides, the tribolayer and matrix are intrinsically identical whether the counterface is hard or soft, as shown in Figures 12(a) and (b).

Under 100 N at 473 K (200 °C), no-oxide tribolayer is similarly formed on worn surfaces (Figure 12(c)).

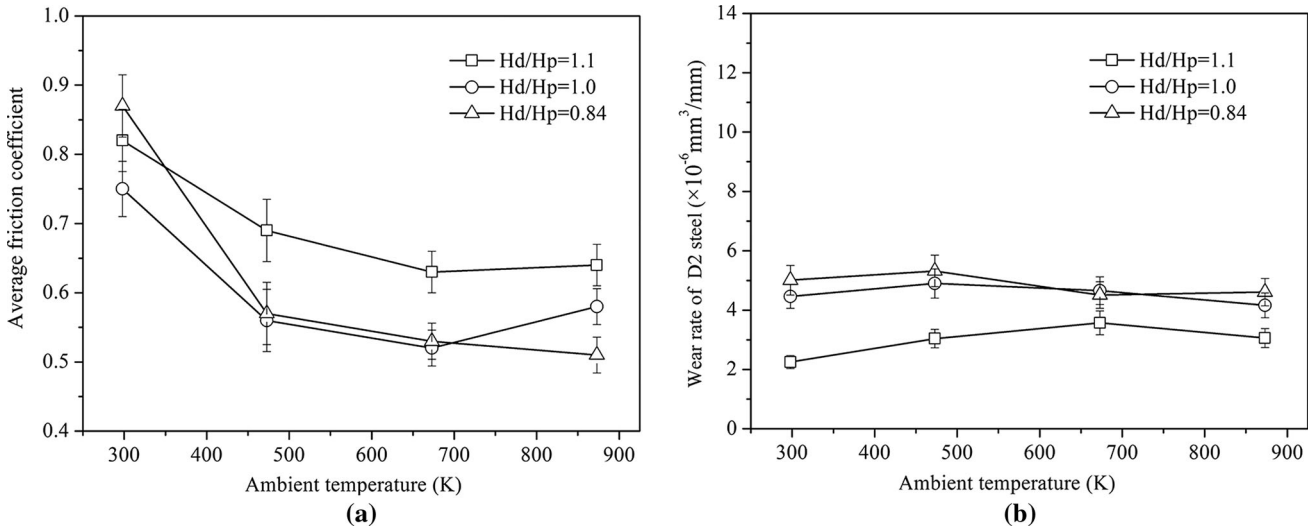

Fig. 13—(*a*) Average friction coefficient and (*b*) wear rate of D2 steel under 300 N.

However, as the ambient temperature and load increase, the flash temperature of worn surface is enhanced, resulting in the reduced oxidation free energy. The tribo-oxides are accelerated to form in tribolayers, which are identified by XRD (Figures 3(b) through (d)). In this case, tribolayer is changed from no-oxide tribolayer to tribo-oxide layer. For $H_d/H_p = 0.84$, tribo-oxide layer is thick, compact, and continuous. Its thickness even reached 5 to 15 μm. Owing to many tribo-oxides, tribo-oxide layers presented high hardness and ceramic characteristics, especially at 673 K and 873 K (400 °C and 600 °C), which are considered to possess a load-carrying capability.[25] Hence, as the layers steadily exist on worn surfaces, the metal-metal contact between the sliding interfaces is avoided. After sliding, merely slight plastic deformation and a few cracks can be found under 300 N, as shown in Figures 12(d), (g), and (j).

For $H_d/H_p = 1.1$, under a light load, the tribo-oxide layer and subsurface remain undamaged and present a similar characteristic to the case of $H_d/H_p = 0.84$. However, under a high load, the tribo-oxide layer becomes unstable. In the research of Stott[22] and Varga,[26] they considered that the soft tissue and material are beneficial to the retention of wear particles and the formation of tribolayers. In other words, it is difficult for the harder surface to form the tribolayer. Furthermore, the smooth tribo-oxide layer, especially containing Fe_2O_3, is believed to possess a self-lubricated function.[27] However, for $H_d/H_p = 1.1$, the counterface with 55 HRC is so hard that less tribo-oxides remain on the worn surfaces. Under the action of load, the hard counterface plows H13 steel pins, resulting in rough worn surfaces. The tribo-oxide layers are readily delaminated; thus, their thickness dramatically decreases. XRD results for $H_d/H_p = 1.1$ confirm that tribo-oxide peaks are always inferior to those of $H_d/H_p = 0.84$ (Figures 3(b) through (d)). In the case of $H_d/H_p = 1.1$, the tribo-oxide layers show unstable existence and, thus, provide an insufficient protective role. When the tribo-oxide layers are totally delaminated, the fresh metal is exposed and the metal-metal contact emerges again. High frictional heat causes thermal softening of H13 steel at 673 K and 873 K (400 °C and 600 °C) (Figure 10(a)). In these cases, severe plastic deformation and many cracks are generated at the subsurface under the action of load. Meanwhile, oxygen immerges into the subsurface along the cracks and oxidizes the metal matrix. Therefore, the multilayer structure is formed, as shown in Figures 12(e), (h), and (k). In spite of the existence of oxides (Figure 10(a)), the multilayer structure was reported to be of no protection, even accelerated wear.[28,29]

Similarly, we can analogize the variation of tribolayer and subsurface for $H_d/H_p = 1$. The tribo-oxide layer is relatively continuous, compact under 300 N at 473 K (200 °C). As the temperature is elevated, the tribo-oxide layer becomes more integrated under a light load, but wreck under a heavy load because of thermal softening of the matrix. Plastic deformation and cracks are noticed, but the degree of deformation and the number of cracks located between those for $H_d/H_p = 1.1$ and 0.84. The evolution process of tribolayers at $H_d/H_p = 1$ is illustrated in Figures 12(f), (i), and (l).

3. *Wear mechanism of steel at different H_d/H_p*

As is well known, the wear behavior and mechanism vary with the test conditions. In the present study, the hardness ratios of disk to pin (H_d/H_p), ambient temperature, and load were used as the main variable parameters of the test conditions. Thus, the wear mechanism is expected to vary as a function of the ambient temperature, load, and counterface hardness. According to XRD analysis results and morphological characteristics of the worn surfaces and subsurfaces, the wear mechanisms of H13 steel at different H_d/H_p can be identified.

As H_d/H_p is 1.1, H13 steel obtains the lowest wear rate at 298 K (25 °C) as well as at 473 K (200 °C) and light load. However, for $H_d/H_p \leq 1$, the wear rate markedly increases. In these cases, all worn surfaces of

H13 steel are characterized by grooves, fish scale, and tearing traces (Figures 4 and 5(a) through (c)). They are typical characteristics of abrasive and adhesive wear.[28–32] Rough worn surfaces usually bring about a large friction coefficient regardless of H_d/H_p, as shown in Figure 13(a). Furthermore, no-oxide tribolayers are noticed to provide the identical role, *i.e.*, no protection, for three hardness ratios. Thus, the counterface hardness, instead of no-oxide tribolayer, mainly decides the magnitude of the wear rate. Archard and Hirst's wear equation about adhesive wear is adequate to explain the wear rate for different H_d/H_p.[2] Clearly, since the sliding distance is identical, the wear is governed by the load and material hardness. For H13 steel, the wear rate increases with the increase in load, but its magnitude is inversely proportional to the counterface hardness (Figures 2(a) and (b)), which is similar to that of the counterface materials (Figure 13(b)).

At 473 K (200 °C) and above, the worn surfaces present totally different morphologies from adhesive wear. In these cases, typical oxidative wear prevails, whose morphology is characterized with smooth tribo-oxide layer and fine oxide particles. Owing to hard tribo-oxides (Fe_2O_3, Fe_3O_4, and FeO), the tribo-oxide layers can possess a load-carrying capability and a protective role. However, there is a prerequisite that the subsurface matrix is able to support the tribo-oxide layers. For $H_d/H_p < 1$, because of the existence of protective tribo-oxide layer at 473 K (200 °C) and above, the wear rate of H13 steel dramatically decreases to (4 to 6) $\times 10^{-6}$ mm^3/mm, even under 300 N. As the temperature is elevated, tribo-oxides further increase and the tribo-oxide layer can remain continuous and compact. Thus, the wear rate both of sliding and counterface materials further decreases at 673 K (400 °C). Kayaba[33] proposed that as the black oxides formed, the wear behavior mainly depended on the oxides, rather than the hardness of materials. However, under 300 N at 873 K (600 °C), high ambient temperature and friction heat softens the H13 steel substrate more or less. The support of H13 steel for tribo-oxide layer is marginally weakened. The wear rate slightly increases but still remains around (4 to 6) $\times$ 10^{-6} mm^3/mm, as shown in Figure 11(d). Therefore, the wear mechanism is considered to be oxidative mild wear. Because of the self-lubricated function of tribo-oxides,[27] the friction coefficient starts to decrease at elevated temperatures, as shown in Figure 13(a).

For $H_d/H_p > 1$, the tribo-oxide layers take effect to decrease the wear rate under light loads. However, under 300 N, the hard counterface readily destroys tribo-oxide layers because of the massive thermal softening of the H13 steel matrix and the abrasive action of counterface. The tribo-oxide layers represent unstable states, such as discontinuous, thin, or even that with the appearance of multilayers. Thus, they do not protect H13 steel from wear. The wear rate linearly increases and the wear resistance markedly deteriorates at elevated temperature. In this case, the harder counterface does not bring about an oxidative mild wear, just as in the works of Bian *et al.*[13] and Viáfara and Sinatora.[15,16] On the contrary, a mild-to-severe transition of oxidative wear prevails at elevated temperatures for $H_d/H_p > 1$. Because of the mutual plowing action, the wear rate of counterface material would also increase at elevated temperatures (Figure 13(b)). For $H_d/H_p = 1$, an appropriate match of the hardness makes the tribo-oxide layer sound and protective, even under 300 N at 473 K (200 °C). Thus, oxidative mild wear prevails in this case. However, at 673 K and 873 K (400 °C and 600 °C), thermal softening of the matrix and high load causes such seriously deformed subsurface as to delaminate tribo-oxide layer, thus increasing the wear rate of H13 steel. The mild-to-severe transition of oxidative wear prevails at 673 K and 873 K (400 °C and 600 °C) as well.

IV. CONCLUSIONS

The dry sliding wear tests of AISI H13 steel (50 HRC) against AISI D2 steel counterface with three hardness levels (55, 50, and 42 HRC) were performed at 298 K to 873 K (25 °C to 600 °C). On the basis of microscopic analysis for worn surfaces and subsurfaces, the relations of H_d/H_p with dry sliding wear behavior and tribo-oxide layers of AISI H13 steel were clarified. The following conclusions are drawn.

1. The different-hardness counterface appreciably changes the wear behavior of H13 steel. For $H_d/H_p > 1$, the wear rate increases with an increase of temperature, but it is roughly inverse for $H_d/H_p < 1$. For $H_d/H_p = 1$, the wear rate first decreases to reach the lowest value at 473 K (200 °C) and then rapidly increases with an increase of temperature. The lowest wear rate of H13 steel appears at 298 K (25 °C) for $H_d/H_p > 1$, at 474 K (200 °C) for $H_d/H_p = 1$, and at 673 K to 873 K (400 °C to 600 °C) for $H_d/H_p < 1$, respectively.
2. Based on the present results, a mild-to-severe wear transition as a function of H_d/H_p roughly complies with Akagaki and Rigney's[14] criterion at room temperature but does not do so at elevated temperatures. Particularly, a mild-to-severe wear transition as a function of H_d/H_p at 673 K to 873 K (400 °C to 600 °C) is against Akagaki and Rigney's criterion.
3. The wear behavior and mechanism of H13 steel are noticed to closely relate with sliding conditions (ambient temperature and load) and H_d/H_p. The acting mechanism of H_d/H_p is by means of its effect on the stability of tribo-oxide layer. Whether the tribo-oxide layers exists stably or not depends on ambient temperature, load, and H_d/H_p, which is considered to be a main factor deciding wear behavior and mechanism.
4. As no-oxide tribolayer exists below 473 K (200 °C), the wear behavior depends on the counterface hardness, which roughly complies with Archard's equation. There is no wear mechanism transition for different-hardness counterfaces. Adhesive and abrasive wear prevail in this case, regardless of any H_d/H_p.
5. As tribo-oxide layer exists at 473 K (200 °C) and

above, the wear depends on the stability of tribo-oxide layer. Oxidative mild wear prevails at 473 K to 873 K (200 °C to 600 °C) for $H_d/H_p < 1$ and merely at 473 K (200 °C) for $H_d/H_p = 1$. However,a mild-to-severe transition of oxidative wear occurs at 473 K to 873 K (200 °C to 600 °C) for $H_d/H_p > 1$ and at 673 K to 873 K (400 °C to 600 °C) for $H_d/H_p = 1$.

ACKNOWLEDGMENTS

Financial support of our work by the National Natural Science Foundation of China (Grant No. 51071078), the Research and Innovation Project for College Graduates of Jiangsu Province (Grant No. KYLX-1031), and the Jiangsu Province Key Laboratory of High-End Structural Materials (Grant No. hsm1403) is gratefully acknowledged.

REFERENCES

1. S.C. Lim and M.F. Ashby: *Acta Metall.*, 1987, vol. 35, pp. 1–24.
2. J.F. Archard and W. Hirst: *Proc. R. Soc. Lond. A*, 1956, vol. 26, pp. 397–410.
3. J.K. Lancaster: *Proc. R. Soc. Lond. A*, 1957, vol. 70B, pp. 112–18.
4. W. Hirst and J.K. Lancaster: *Proc. R. Soc. Lond. A*, 1960, vol. 259A, pp. 228–41.
5. J.L. Sullivan and S.S. Athnal: *Tribol. Int.*, 1983, vol. 64 (3), pp. 123–31.
6. D.K. Chaudhuri, A.J. Slifka, and J.D. Siegwarth: *Wear*, 1993, vol. 160, pp. 37–50.
7. Y. Wang and T.Q. Lei: *Wear*, 1996, vol. 194, pp. 44–53.
8. G. Straffelini, D. Trabucco, and A. Molinari: *Metall. Mater. Trans. A*, 2002, vol. 33A, pp. 613–24.
9. D. Rai, B. Singh, and J. Singh: *Wear*, 2007, vol. 263, pp. 821–29.
10. V. Abouei, H. Saghafian, and S. Kheirandish: *Wear*, 2007, vol. 262, pp. 1225–31.
11. H. So, H.M. Chen, and L.W. Chen: *Wear*, 2008, vol. 265, pp. 1142–48.
12. F. Velasco, M.A. Martinez, R. Calabres, A. Bautista, and J. Abenojar: *Tribol. Int.*, 2009, vol. 42, pp. 1199–1205.
13. S. Bian, S. Maj, and D.W. Borland: *Wear*, 1993, vol. 166, pp. 1–5.
14. T. Akagaki and D.A. Rigney: *Wear*, 1991, vol. 149, pp. 353 74.
15. C.C. Viáfara and A. Sinatora: *Wear*, 2009, vol. 267, pp. 425–32.
16. C.C. Viáfara and A. Sinatora: *Lubr. Sci.*, 2013, vol. 25, pp. 123–38.
17. M. Roy, A. Pauschitz, J. Wernisch, and F. Franek: *Mater. Corros.*, 2004, vol. 55 (4), pp. 259–71.
18. J. Zhang and A.T. Alpas: *Acta Mater.*, 1997, vol. 45, pp. 513–28.
19. Y. Wang, T.Q. Lei, and J.J. Liu: *Wear*, 1999, vol. 231, pp. 1–11.
20. J.E. Wilson, F.H. Stott, and G.C. Wood: *Proc. R. Soc. London A*, 1980, vol. 369, pp. 557–74.
21. F.H. Stott: *Tribol. Int.*, 2002, vol. 35, pp. 489–95.
22. F.H. Stott and M.P. Jordan: *Wear*, 2001, vol. 250, pp. 391–400.
23. O. Barrau, C. Boher, R. Gras, and F. Rezai-Aria: *Wear*, 2003, vol. 255, pp. 1444–54.
24. S.Q. Wang, M.X. Wei, F. Wang, X.H. Cui, and C. Dong: *Tribol. Lett.*, 2008, vol. 32, pp. 67–72.
25. C. Colombia, Y. Berthier, A. Floquet, L. Vincent, and M. Godot: *J. Tribol. Trans. ASME*, 1984, vol. 106, pp. 194–201.
26. M. Varga, H. Rojacz, H. Winkelmann, H. Mayer, and E. Badisch: *Tribol. Int.*, 2013, vol. 65, pp. 190–99.
27. H. Kato: *Wear*, 2003, vol. 255, pp. 426–29.
28. M.X. Wei, S.Q. Wang, L. Wang, X.H. Cui, and K.M. Chen: *Tribol. Int.*, 2011, vol. 44, pp. 898–905.
29. Q.Y. Zhang, K.M. Chen, L. Wang, X.H. Cui, and S.Q. Wang: *Tribol. Int.*, 2013, vol. 61, pp. 214–23.
30. L. Wang, Q.Y. Zhang, X.X. Li, X.H. Cui, and S.Q. Wang: *Metall. Mater. Trans. A*, 2014, vol. 45A, pp. 2284–96.
31. K.M. Chen, Y. Zhou, X.X. Li, Q.Y. Zhang, L. Wang, and S.Q. Wang: *Mater. Des.*, 2015, vol. 65, pp. 65–73.
32. L. Wang, Q.Y. Zhang, X.X. Li, X.H. Cui, and S.Q. Wang: *Tribol. Lett.*, 2014, vol. 53, pp. 511–20.
33. T. Kayaba and A. Iwabuchi: *Wear*, 1981, vol. 66, pp. 27–41.